

Effect of heat exchanger base thickness and cooling fan on cooling performance of Air-To-Air thermoelectric refrigerator; experimental and numerical study

Faraz Afshari ^{*}, Mehmet Akif Ceviz, Emre Mandev, Fatih Yıldız

Erzurum Technical University, Department of Mechanical Engineering, Erzurum, Turkey



ARTICLE INFO

Keywords:
Thermoelectric
Heat exchanger
COP
Refrigerators
Optimization

ABSTRACT

The available statistics reveal that a significant portion of the total electrical energy in different communities is used for various heating and cooling purposes and refrigeration in the domestic and industrial sectors, which includes cooling systems in critical areas such as the food and pharmaceutical industries. In this work, air-to-air thermoelectric cooling systems have been analyzed. Experimental and numerical attempts have been made to evaluate the influence of the base thickness size of external heat exchanger on cooling performance of refrigerator. In addition, the cooling system has been operated in different working conditions and the effect of cooling fan velocity on the Coefficient of Performance (COP) value was presented. It was found revealed that, the temperature of the cooling chamber for 4.5 mm thickness dropped to 11.57 °C, while this temperature was 9.93 °C for 1.5 mm thickness. Considering the final temperatures, there was a 14% difference by reducing the thickness from 4.5 mm to 1.5 mm for the case of $V_{air} = 7.5$ external fan speed. For the numerical approach, ANSYS Fluent 16.0 software was utilized to analyze the structure of airflow inside and outside of the refrigerator in detail. As a result of Computational Fluid Dynamics (CFD) simulation temperature distribution and air velocity contours have been obtained and achieved results were discussed.

Introduction

Cooling systems and refrigerators are widely used in air conditioning as well as storage of medicine, food and fruit. Studies and researches on the subject of cooling systems are a significant issue in energy saving. No matter how small this energy saving is for a cooling device, considering its worldwide and wide use, a huge energy saving will occur. In this context, vapor compression cooling systems and refrigerators have a notable impact on the sector due to their high performance [1]. However, these systems have a complex structure and are noisy, and their volume is large and heavy. As a result, thermoelectric cooling systems can be proposed as an appropriate alternate for vapor compression systems. Having no mechanical moving parts and no working fluid, lightweight, fast thermal response, high reliability, silent operation and compact structure make them attractive to use as mini refrigerator for storing food and medicine in various conditions especially emergencies such as refugee camps [2]. The Peltier effect is also well known in the fields of thermal analysis, calorimetry and calibration and heat flow compensation. Cooling systems based on the Peltier effect are now used

for the design and manufacturing of microcalorimeters and PC processors [3].

Many valuable research in the field of Peltier cooling devices have been presented in articles with the aim of improving performance and efficiency and evaluating optimal working conditions [2,4,5]. Abdul-Wahab et al. [6] investigate thermoelectric refrigerators operated by solar energy to use in desert conditions in which electricity is not available. These types of refrigerators were proposed as convenient systems to use in unfavorable difficult conditions. Experimental and numerical studies were performed to compare performance of air-to-water with air-to-air Peltier cooling systems considering COP values. Additionally, heating and cooling rate of the TE systems were analyzed and the models were simulated using CFD methods [7,8]. In a study, Chen, et al. [9] surveyed the efficiency of the TE power cycle to combined heat and power production systems. It was concluded that the integration of thermoelectric into energy systems, especially combined heat and power production can be considered as an efficient solution for energy saving.

TE refrigerators powered by solar cells were investigated by Dai et al. [10] experimentally. The system can be operated at night and day using

* Corresponding author.

E-mail address: faraz.afshari@erzurum.edu.tr (F. Afshari).

Nomenclature	
C_p	Specific heat capacity (J/kg K)
COP	Coefficient of performance
I	Electric current (A)
h	Average forced-convection coefficient ($\text{W}/\text{m}^2 \text{K}$)
k	Thermal conductivity (W/mK)
K	Turbulent kinetic energy (J/kg)
m	Mass (kg)
\dot{m}	Flow rate (kg/s)
p	Pressure (Pa)
\dot{Q}	Heat transfer rate (W)
Q	Heat transfer (J)
T	Temperature ($^\circ\text{C}$)
t	Time (s)
TE	Thermoelectric
TEC	Thermoelectric cooler
U_c	Uncertainty
V	Voltage (V)
v	Volume (m^3)
v	Air velocity (m/s)
W	Power consumption (W)
ρ	Density (kg/m)
C_μ	Turbulence constant
ϵ	Turbulent dissipation rate (m^2/s^3)
μ	Dynamic viscosity (kg/m s)
μ_t	Turbulent viscosity (kg/m s)
Subscripts	
f	Fan
h	Hot side
c	Cold side
pe	Peltier
∞	Free stream or ambient

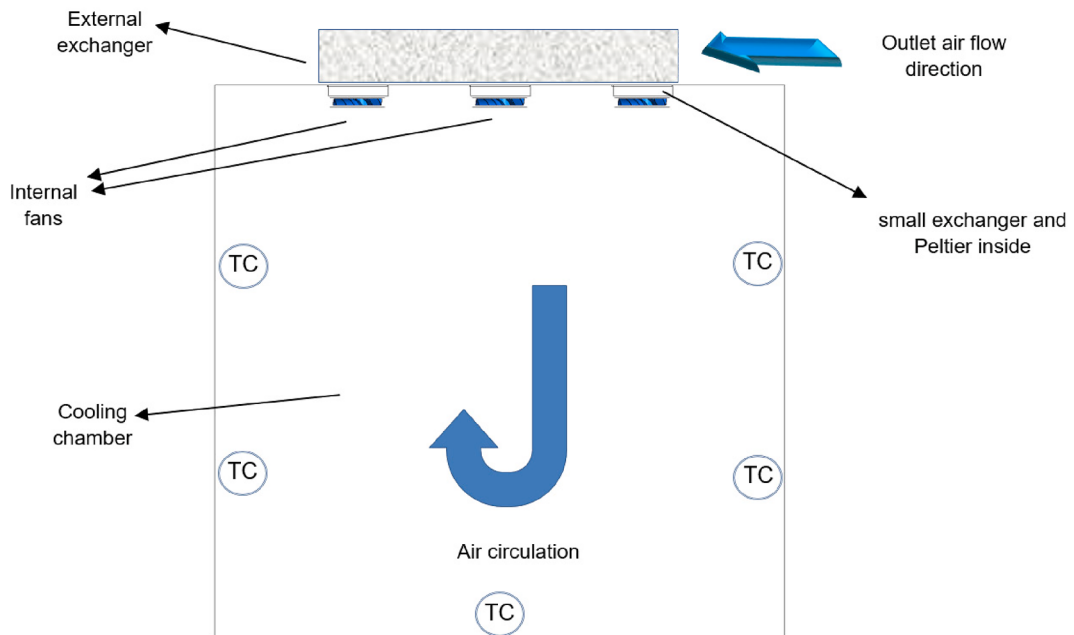


Fig. 1. Schematic view of manufactured air-to-air cooling system.

a storage battery assisted by a rectifier, which makes the proposed refrigerator portable and useful. Storage battery was utilized to provide required electrical power in night and cloudy days. In a research, Gong et al., analyzed thermo-mechanical efficiency of a compact TE cooling system. Modeling of the cooling system was performed using finite element method considering the system works in a temperature-dependent conditions. The effects of thermal load applied electrical current, leg length and ceramic plate on the performance were examined [11].

Tian et al. [12] conducted a study on tubular thermoelectric module using tube-bundle arrangement for an air cooler device. Additionally, geometric properties of tubular TEs were examined and the efficiency of the proposed system was discussed. For low-temperature applications, Ali et al. [13] conducted a computational study of transverse TE coolers. It was revealed that, by applying intermediate currents the maximum temperature depression will be produced. The impact of significant parameters such as tilt angle and device aspect ratio were examined and optimization of the parameters was performed. TE cooling systems are

widely used for cooling electronic devices. In this context, design optimization was carried out for TE coolers proposed to use in cooling electronic elements. The finite thermal conductance between the heat exchangers located at hot and cold sides of the TEC was considered and the constraint of the total thermal conductance was evaluated [5]. It has been stated that thermoelectricity can be used in buildings to meet indoor thermal needs as well as refrigerators. Martín-Gómez et al. [14] studied on integrated ventilated active TE envelope to evaluate thermal performance of the proposed system. The optimal design and construction of ventilated active TE envelope prototypes were analyzed and it was revealed that these systems can be considered as an alternative solution for both cooling and heating in zero energy buildings. Liu et al. [15] conducted a review study on existing solar TE cooling technologies to employ in the zero energy buildings to obtain a clear state of the solar TE cooling technologies. It was proposed that, the technical route of the mentioned technologies can be considered to use in zero energy buildings. Phase-change materials and thermoelectric hybrid generators have been proposed as novel methods to increase performance of

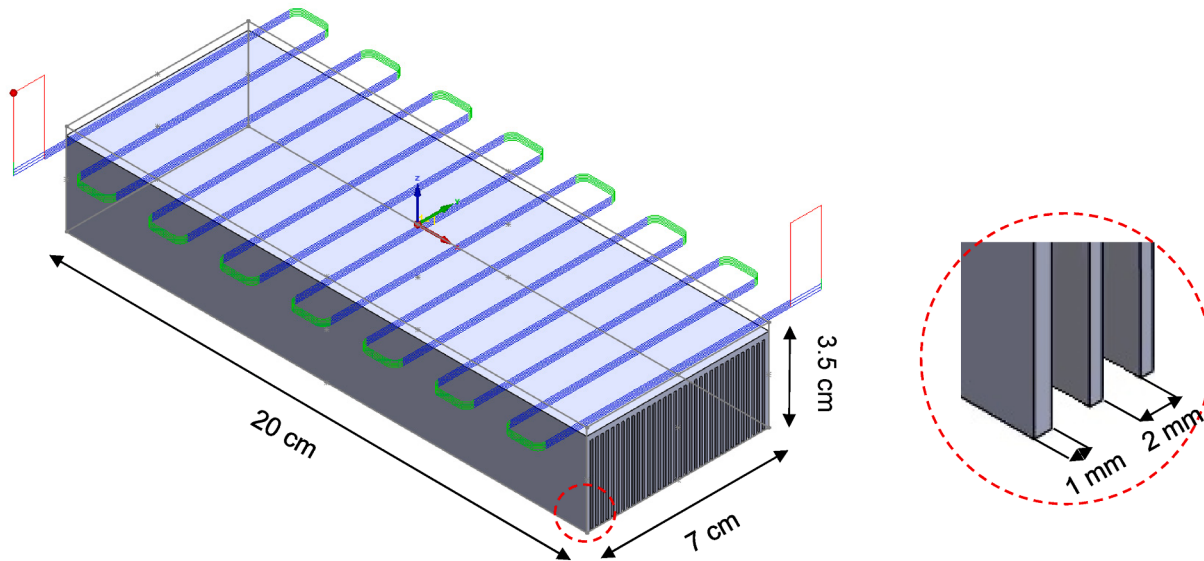


Fig. 2. Presentation of the stock-target models and tool paths defined in CAM programming with sizes and details.

Table 1
Test plan of this present study.

Base Thickness (mm)	Velocity (m/s)	TEC Energy Consumption (W)	Time (s)
1.5	7.5	90	1500
	15		
	20		
	30		
3.0	7.5	90	1500
	15		
	20		
	30		
4.5	7.5	90	1500
	15		
	20		
	30		

thermoelectric coolers [16,17]. Moreover, separated-configured arrangement of micro-thermoelectric coolers has been also proposed, which was modeled by using mathematical methods by Liu et al. [18]. Experimental and numerical analyses were performed by Zhou et al. [19] to evaluate performance of a two-stage indirect-thermoelectric cooling system. The effects of several parameters on the operation of the system were examined and a mathematical model for the proposed system was developed. Performance analysis was made for a loop heat pipe combined with TE cooling device and operating conditions were examined experimentally under acceleration field. The influence of acceleration magnitudes on efficiency of loop heat pipe was discussed [20]. Wang et al. designed a cooling system based on Peltier effect combined with electrohydrodynamics. In the proposed cooling device, a single heat-sink was proposed and the optimization research was done for the combined system using thermodynamic methods. In this study, the photoelectric specifications of a LED chip were also improved [21].

In addition to the literature knowledge given above, when other studies in this field are examined, it becomes clear that the geometric properties of finned heat exchangers in TE cooling systems and their effects on the flow and heat transfer performance resulting from the change of these properties have not been adequately examined. With regard to this issue, the innovation of this research is the design of a new type of vertical finned heat exchanger in the external part of the cooling system to increase the efficiency of the device, which has been supported by airflow between the fins and optimization experiments on airflow velocity. Additionally, paying less attention to the heat exchanger base

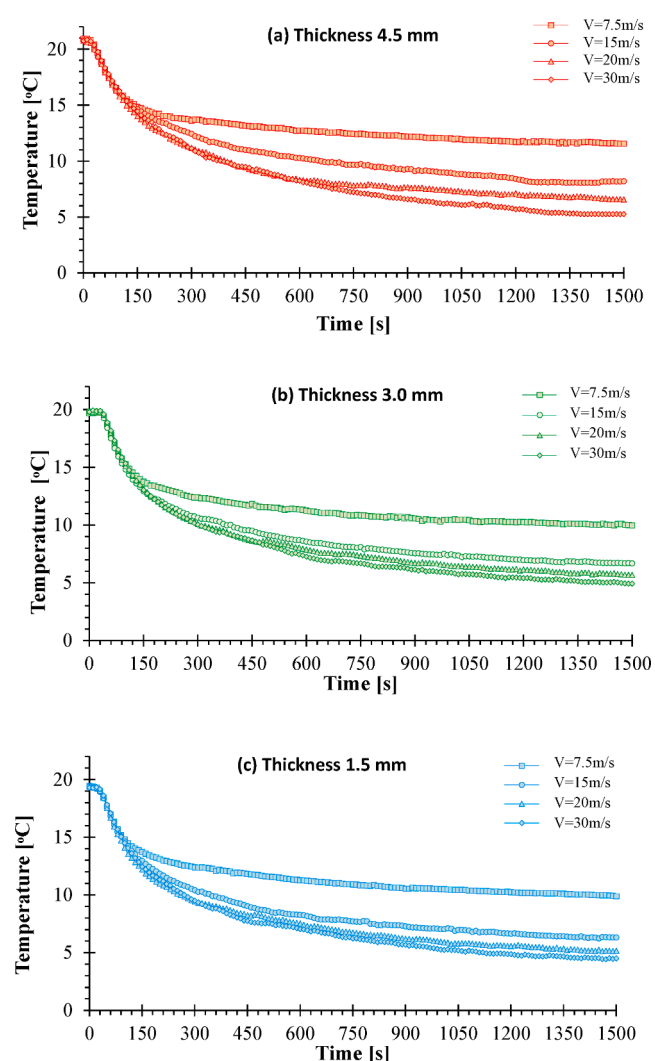


Fig. 3. Temperature variation with test time for three different thicknesses of the exchanger base.

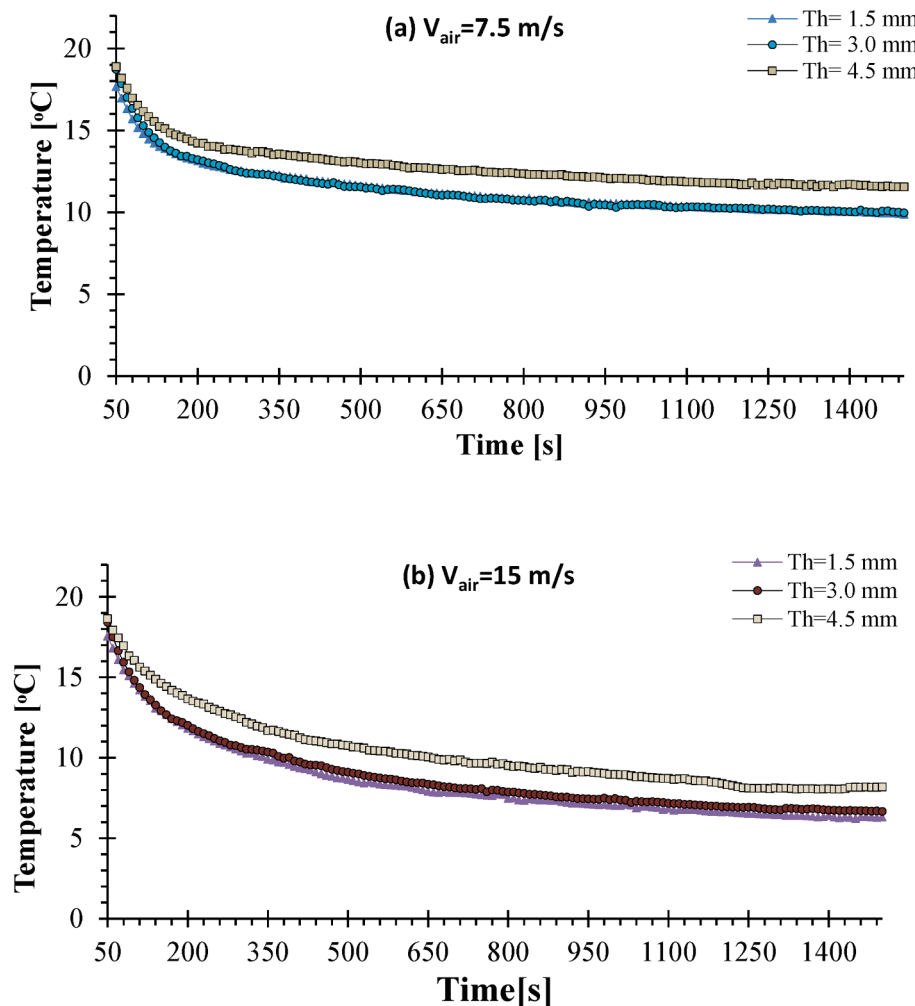


Fig. 4. Temperature variation with test time at air velocity of $V_{\text{air}} = 7.5$ and 15 m/s .

thickness, which is an important factor in the performance and heat transfer rate, is the main gap in studies over TE cooling systems. This present study aims to pay attention in detail to evaluate the effect of the heat exchanger base thickness. Therefore, thermoelectric cooling devices have been investigated by experimental and numerical methods to reveal effects of heat exchanger base thickness on COP value of the TE air-to-air cooling system. Additionally, influence of external cooling fan and air velocity on the performance has been evaluated. CFD simulation results have been provided using ANSYS/Fluent software and temperature distribution and flow structure have been analyzed in both external and internal domains.

Experimental procedure details

In this study, a laboratory-scale styrofoam cooling chamber with an interior volume of 0.022506 m^3 was used to analyze the effects of fan velocities and exchanger base thicknesses on performance of TEC cooling module. The experiments were performed on an air-to-air cooling system. The details of the cooling chamber are demonstrated in Fig. 1. Heat exchangers, as an important part of energy-based application systems, play an important role in heating and cooling devices [22–26], which must be properly selected to achieve the highest performance to transfer heat from the source to the designated destination. On both cold and hot sides of the system, suitable heat exchangers were installed and air fans were placed to increase heat transfer in the exchangers.

A powerful fan for the external heat exchanger and smaller fans

inside cooling chamber were used to transfer heat from the exchangers to the environment. One external heat exchanger and three internals were installed inside the system. The dimensions of the internal and external heat exchangers are $4 \times 4 \times 1 \text{ cm}$ and $20 \times 7 \times 3.5 \text{ cm}$, respectively. The base thickness of the external heat exchangers was thinned in two stages to be 1.5 mm , 3 mm and 4.5 mm . In this context, Haas-VF2 CNC vertical machining center was used to thin the base of the external heat exchangers. CNC programming was carried out using the SolidCAM milling software. 63 mm diameter tungsten carbide face milling tool was used for milling operation. As the cutting parameter, the spindle speed was 2500 rpm , the feed rate in the X-Y plane was 1000 mm/min and cutting depth was 0.5 mm . The stock-target model and tool paths defined in the program were given in Fig. 2. Between connected surfaces (Peltier surfaces and exchangers) high thermal conductivity grease HY510 was used to improve heat transfer effectively. The dimension of used Peltier module (TEC1-12715) is $40 \times 40 \times 4 \text{ mm}$. The experiments were carried out using three Peltier TEs inside cooling chamber. During the tests, temperature variations inside the cooling chamber were analyzed using a high quality thermal camera under the brand name TESTO 885-2 Thermal Imager. The measuring range of the utilized camera is between $-30 \text{ }^{\circ}\text{C}$ and $+350 \text{ }^{\circ}\text{C}$, with accuracy and thermal sensitivity of $\pm 2 \text{ }^{\circ}\text{C}$ and $<30 \text{ mK}$ at $30 \text{ }^{\circ}\text{C}$, respectively. Variations of the temperature inside cooling chambers were recorded along a center line using five K-type thermocouples and a data logger over test time. The data obtained from the cooling chambers have been transferred to the computer by using a Hioki LR8402-20 model data logger.

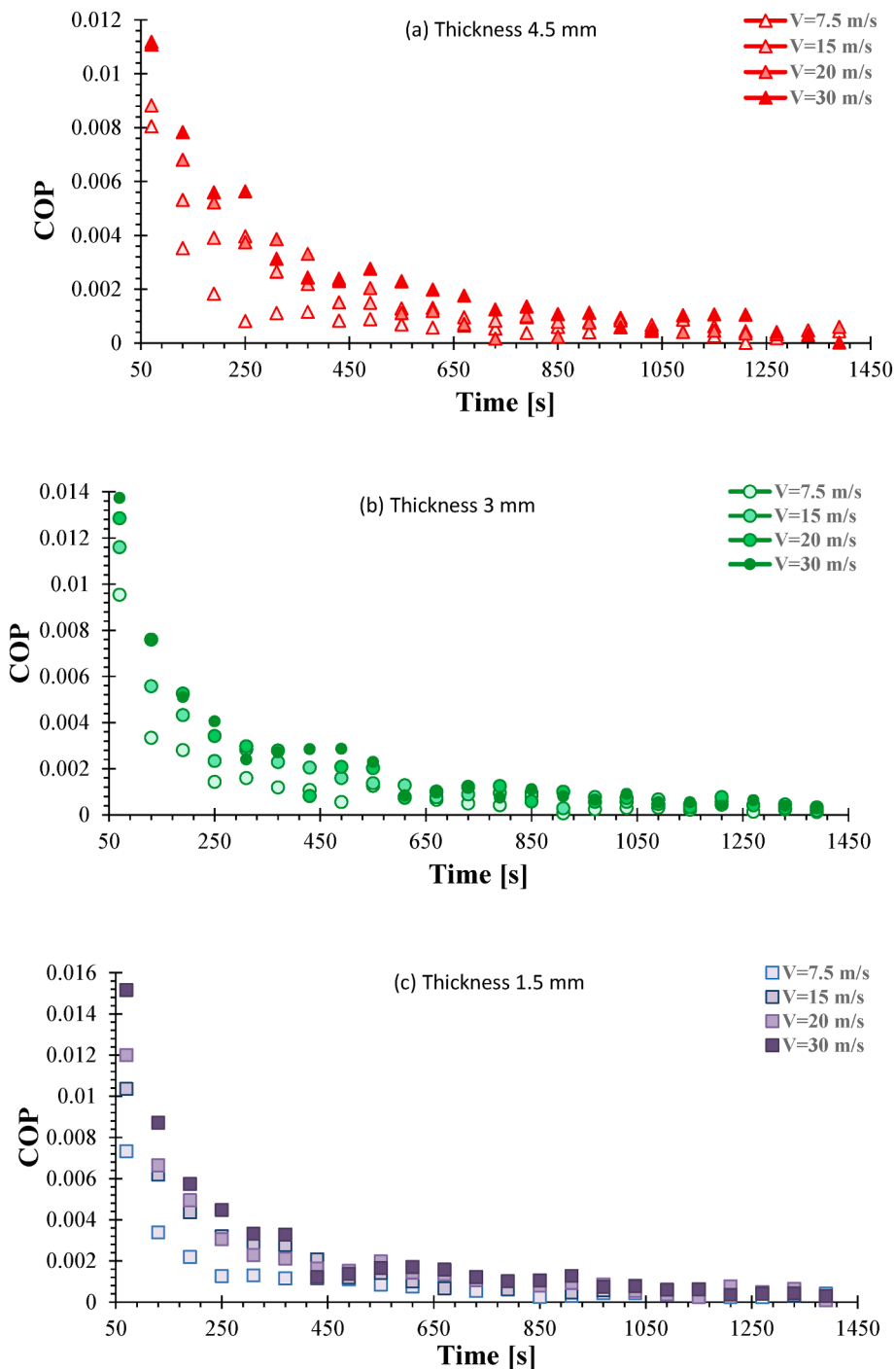


Fig. 5. COP variations during test time for three different thicknesses of the exchanger base.

with 0.01 °C resolution. The working temperature of the used thermocouples is -20 °C to 100 °C and their measurement accuracy is 0.01 °C. Thermocouples have been calibrated at intervals of 3 °C between 1 and 49 °C and calibration curves were generated and used in the calculations. The selected time for temperature measurements is 1500 s. In the analysis and calculations, the average temperature inside the refrigerator was calculated and in addition, current and voltage values were recorded to calculate the power consumption of the TE Peltier cooling device. Table 1 has been presented to display the test plan performed in this present work.

Numerical approach

Numerical approach was performed by modeling three Peltiers in serial form to analyze cooling performance of the refrigerator. The under evaluation refrigerator thermodynamically has been optimized and its COP value was obtained in different operating conditions. The model of the refrigerator was simulated exactly according to the experimental conditions in the same dimensions. In the center of the refrigerator, the air circulation created by the three fans is displayed by an arrow. ANSYS fluent 16 software was employed in the numerical approach and drawing of geometries, mesh process, boundary conditions and solution were performed respectively for a cooling chamber with dimensions of

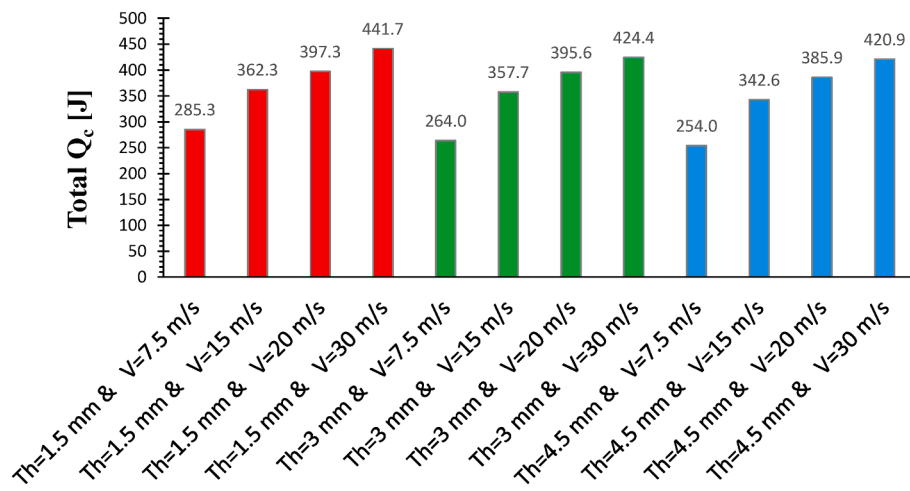


Fig. 6. Total cooling load (Q_c) for different heat exchanger base thickness at various air velocities (7.5, 15, 20, and 30 m/s).

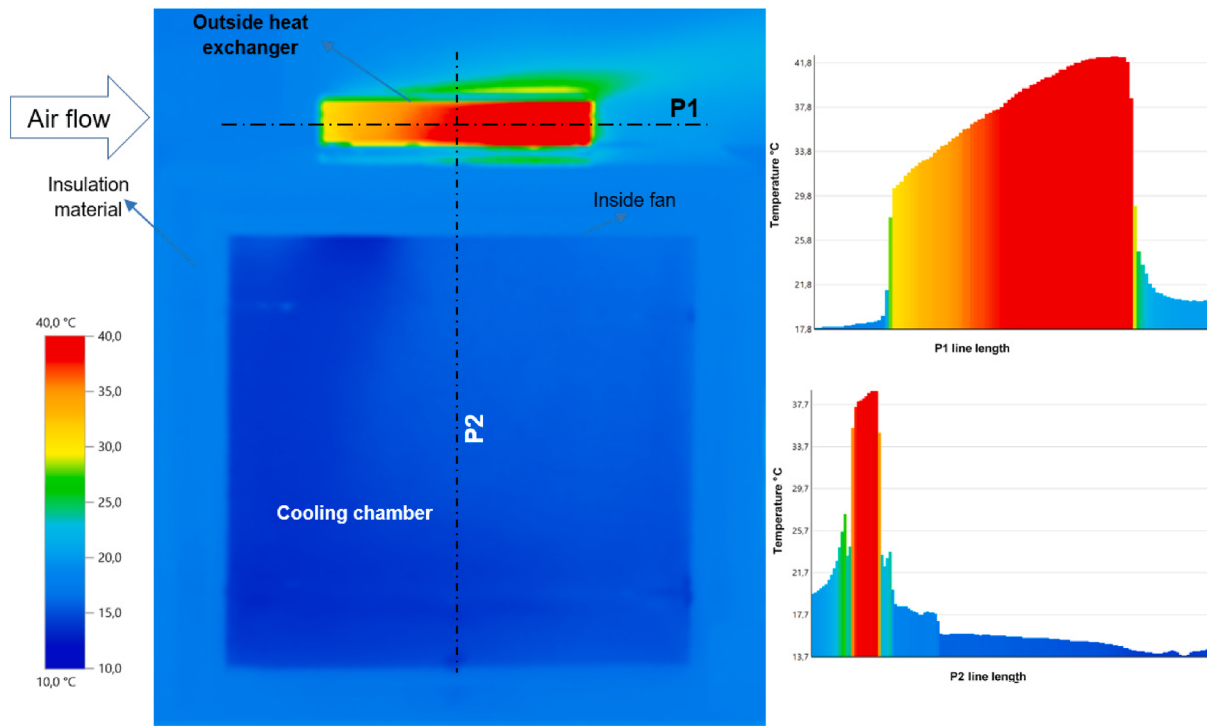


Fig. 7. Temperature distribution inside cooling chamber and external heat exchanger and the position of the P1 and P2 lines.

$43 \times 41 \times 26$ cm. In the solutions, it was assumed that the cooling chamber was insulated and the walls are closed to heat transfer.

The internal fans and air circulation, external heat exchanger, Peltier positions and fitted heat exchangers inside have been also shown in the Fig. 1. It should be noted that, in the solution process for the mentioned problem a time-dependent method was due to the continuous change in the situations and temperature of the refrigerator.

In the mesh process, the quality of applied mesh has been considered carefully and the obtained results were analyzed to achieve the optimum mesh number and geometry. More compact and finer meshes were considered near the walls and areas near the boundaries. Moreover, curvature mode with a growth rate of 1.2 was performed in the mesh generation process. The skewness value specified in the mesh generation is a significant parameter that represents the mesh quality. In the numerical work, average and maximum skewness values of the refrigerator were 0.24 and 0.89 respectively.

Momentum, continuity and energy equations are the main governing equations in CFD simulation and solution of the problem [29], which are presented respectively as,

Momentum equation:

$$\nabla \cdot (\rho \vec{v}) = -\nabla p + \nabla \cdot (\mu \left[(\nabla \vec{v} + \nabla \vec{v}^T) - \frac{2}{3} \nabla \cdot \vec{v} I \right]) \quad (1)$$

Continuity equation:

$$\nabla \cdot (\rho \vec{v}) = 0 \quad (2)$$

Energy conservation balance:

$$\nabla \cdot (\vec{V}(\rho E + p)) = \nabla \cdot k_{eff} \nabla T - h \vec{J} + (\mu \left[(\nabla \vec{v} + \nabla \vec{v}^T) - \frac{2}{3} \nabla \cdot \vec{v} I \right] \cdot \vec{v}) \quad (3)$$

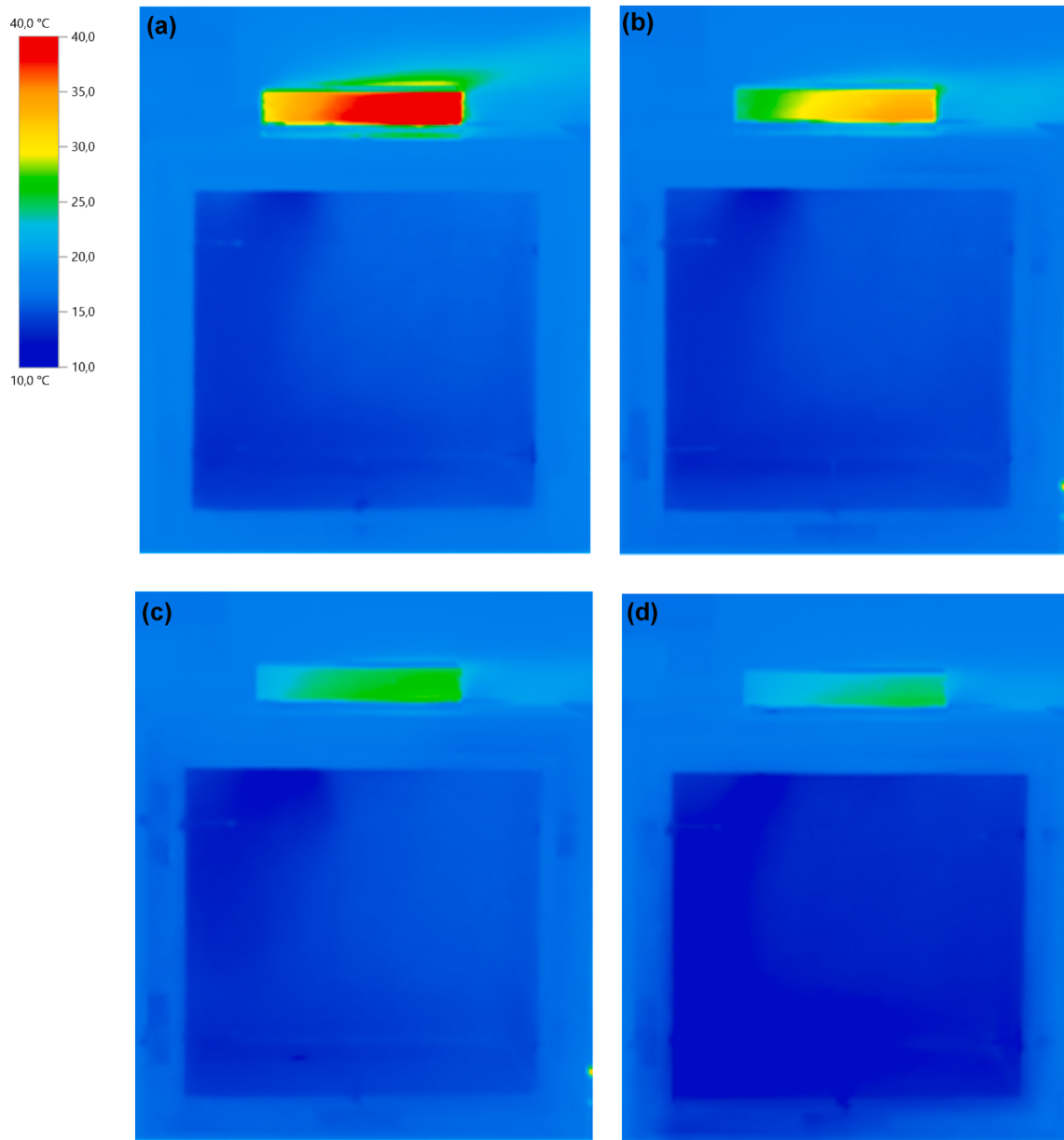


Fig. 8. Temperature distribution inside cooling chamber and heat exchanger at air velocity of 7.5 m/s (a), 15 m/s (b), 20 m/s (c), and 30 m/s (d).

The k- ϵ model is a numerical methodology that is widely employed (especially in turbulent flows) to solve CFD problems. The k- ϵ equations are presented as following equations,

$$\frac{\partial}{\partial x_i} \left(\left(\frac{\mu_t}{\sigma_k} + \mu \right) \frac{\partial k}{\partial x_j} \right) - (\rho \epsilon) + G_k = \frac{\partial}{\partial x_i} [(u_i \rho k)] \quad (4)$$

$$\frac{\partial}{\partial x_i} (u_i \rho \epsilon) = \frac{\partial}{\partial x_j} \left[\left(\frac{\mu_t}{\sigma_\epsilon} + \mu \right) \frac{\partial \epsilon}{\partial x_j} \right] + \left(\frac{\epsilon}{k} G_k C_{1\epsilon} \right) - \left(\rho \frac{\epsilon^2}{k} C_{2\epsilon} \right) \quad (5)$$

$$\mu_t = \rho C_\mu \frac{k^2}{\epsilon} \quad (6)$$

$$G_k = - \frac{\partial u_j}{\partial x_i} \rho \bar{u}_j \bar{u}_i \quad (7)$$

Analysis and calculations

COP value of the heating and cooling systems represents the system

efficiency and is known as one of the most significant part of analysis in these systems, which is also calculated for refrigerators and thermo-electric systems. In this regard, thermodynamic equations can be employed to obtain the total amount of COP by dividing heat (Q_c) transferred from cooling chamber of refrigerator by total consumed power. This equation is presented in Eq. (8). In this equation, the electrical power consumption by Peltier TE and fan elements has been taken into consideration as follows,

$$COP_{Total} = \frac{Q_c}{W_{pe} + W_f} \quad (8)$$

Electrical power consumption of the elements is calculated by following equation as,

$$W = VI \times t \quad (9)$$

Here V and I indicate the values of voltage and electrical current. In the calculation air mass inside cooling chamber should be calculated. Air mass amount inside the cooling chamber can be expressed having the

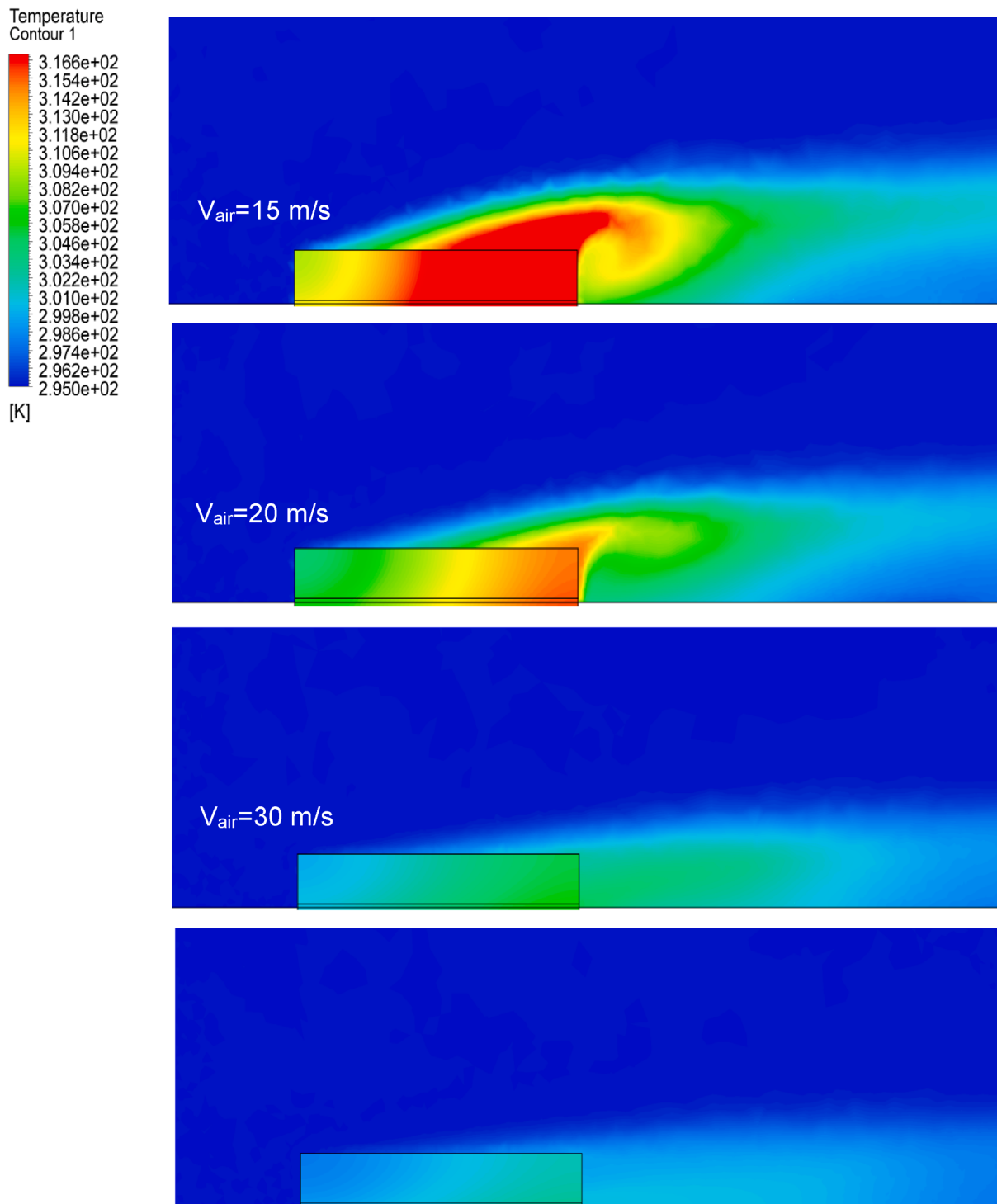


Fig. 9. Temperature contours of the external heat exchanger (side view).

volume of the cooling chamber (0.022506 m^3) and density of the air inside,

$$m = \rho v \quad (10)$$

The heat transferred from the cooling chamber to the environment can be calculated by Eq. (11) [27] as,

$$Q_c = mC_{p,air}[T_{2,air} - T_{1,air}] \quad (11)$$

In Eq. (11), T_1 and T_2 are the first and last mean temperatures of the cooling chamber during test time and m is the mass of air inside

calculated in Equation (10). It should be stated that, temperature of the cooling chamber was obtained using five thermocouples inside and the mean temperature was calculated to use in analyses. Heat transfer by cooling air at outside (upper parts of the cooling chamber) can be calculated as,

$$Q_h = \dot{Q}_h \times t = [\dot{m}C_{p,air}(T_{2,air} - T_{1,air})] \times t \quad (12)$$

Error rate in analysis may result from different parameters including instrument selection, observation, calibration, scheduling, reading, and sometimes environmental errors. In this regard, error analysis should be

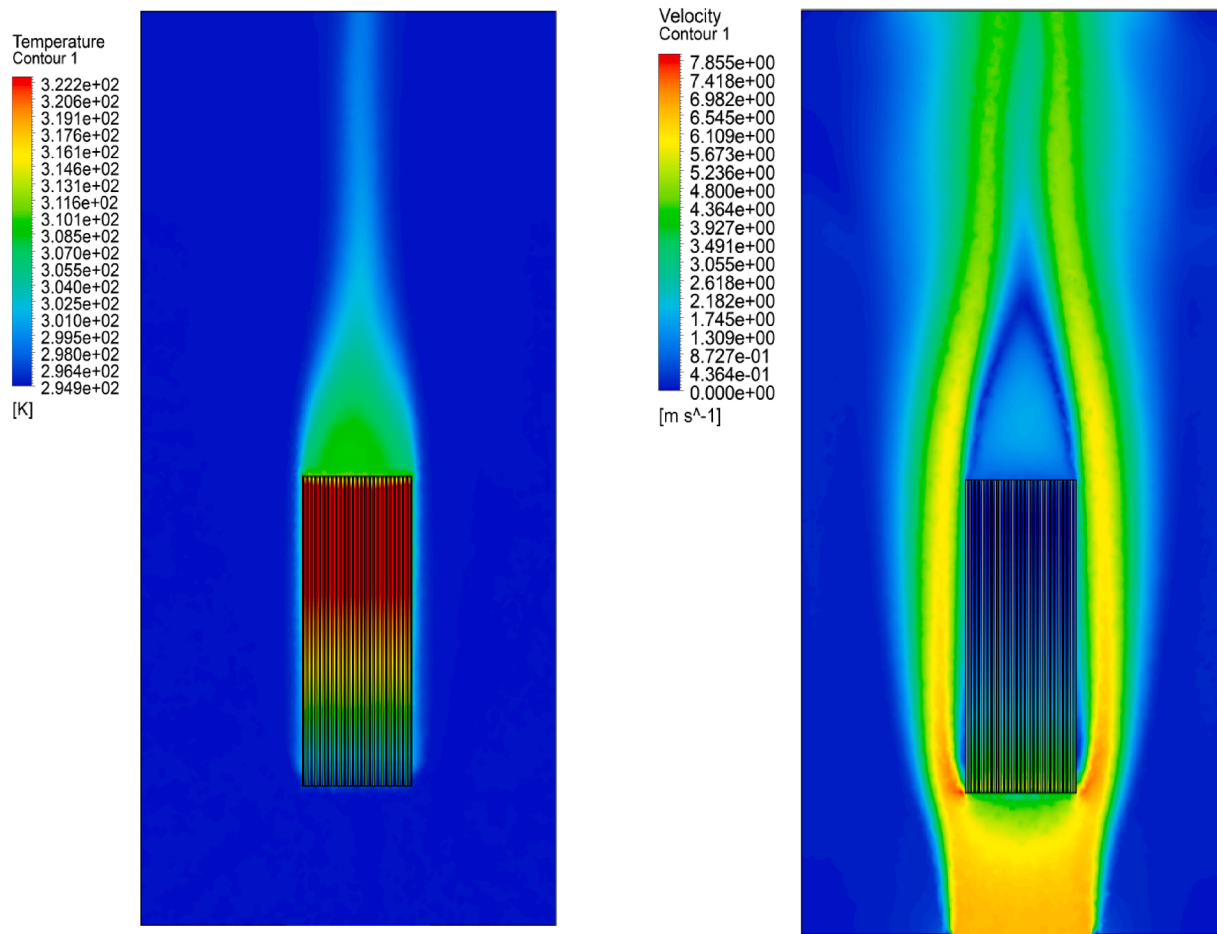


Fig. 10. Temperature and velocity contours of the external heat exchanger (top view) at $V_{\text{air}} = 7.5 \text{ m/s}$.

performed in experimentally measured values, which can be presented in the form of mathematical relationship. Generally, if the output quantity B is assumed to be calculated from input values A_1, A_2, \dots, A_n according to a function as $B = F(A_1, A_2, \dots, A_n)$, the combined uncertainty of the output quantity $u_c(b)$ can be obtained by uncertainties of the input data $u(a_i)$ as follows [28],

$$u_c(y) = \sqrt{\left[\frac{\partial Y}{\partial X_1} u(x_1)\right]^2 + \left[\frac{\partial Y}{\partial X_2} u(x_2)\right]^2 + \dots + \left[\frac{\partial Y}{\partial X_n} u(x_n)\right]^2} \quad (13)$$

As it is known, the COP value is a function of energy consumed by TEC and cooling rate of refrigerator. So the uncertainty of TEC performance can be computed by the following equation, from which the obtained uncertainty for COP was $\pm 2.8\%$.

$$U_c(\text{COP}) = \sqrt{\left(U_T \frac{\partial \text{COP}}{\partial T_{\text{coolingchamber}(1)}}\right)^2 + \left(U_T \frac{\partial \text{COP}}{\partial T_{\text{coolingchamber}(2)}}\right)^2 + \left(U_w \frac{\partial \text{COP}}{\partial \dot{W}}\right)^2} \quad (14)$$

Results and discussion

In this section, the experimental results are evaluated and the average cooling chamber temperatures, COP and total cooling load (Q_c) values are obtained and discussions on the diagrams and contours are presented. By using the ANSYS-Fluent package program, CFD results are given as velocity and temperature contours.

Experimental results

In Fig. 3, the temperature change of the cooling chamber is presented depending on test time. Fig. 3(a) represents the results for the heat exchanger with a base thickness of 4.5 mm, while (b) and (c) are for heat exchangers with a base thickness of 3.0 and 1.5 mm, respectively. In each diagram, different external fan velocity results have been compared at $V_{\text{air}} = 7.5, 15, 20$, and 30 m/s .

The temperature value of the ambient was approximately 20°C , and the temperature of external heat exchanger changes depending on the external fan speed. In addition, the temperature differences in the cooling chamber for all cases changed significantly after approximately 150 s. From the obtained results, the lowest cooling chamber temperature was obtained as 4.5°C for 1.5 mm heat exchanger base thickness and $V_{\text{air}} = 30 \text{ m/s}$.

In Fig. 4, the variation of cooling chamber temperatures over time at heat exchanger base thicknesses of $V_{\text{air}} = 7.5$ and $V_{\text{air}} = 15 \text{ m/s}$, is presented. Here, a significant difference in temperatures is observed by decreasing the heat exchanger base thickness from 4.5 mm to 3.0 mm. However, this difference is considerably lower in the heat exchanger base thickness reduced from 3 mm to 1.5 mm. In Fig. 4(a), the temperature of the cooling chamber for 4.5 mm thickness has dropped to 11.57°C , while this temperature is 9.93°C for 1.5 mm thickness. Considering the final temperatures, there is a 14% difference by reducing the thickness from 4.5 mm to 1.5 mm for the case of $V_{\text{air}} = 7.5 \text{ m/s}$ external fan speed. A similar situation is also observed for $V_{\text{air}} = 15 \text{ m/s}$ external fan speed. For this reason, it has been concluded that more effective cooling can be achieved by reducing the heat exchanger thickness. In cases where the external fan speed is high, ($V_{\text{air}} = 20$ and

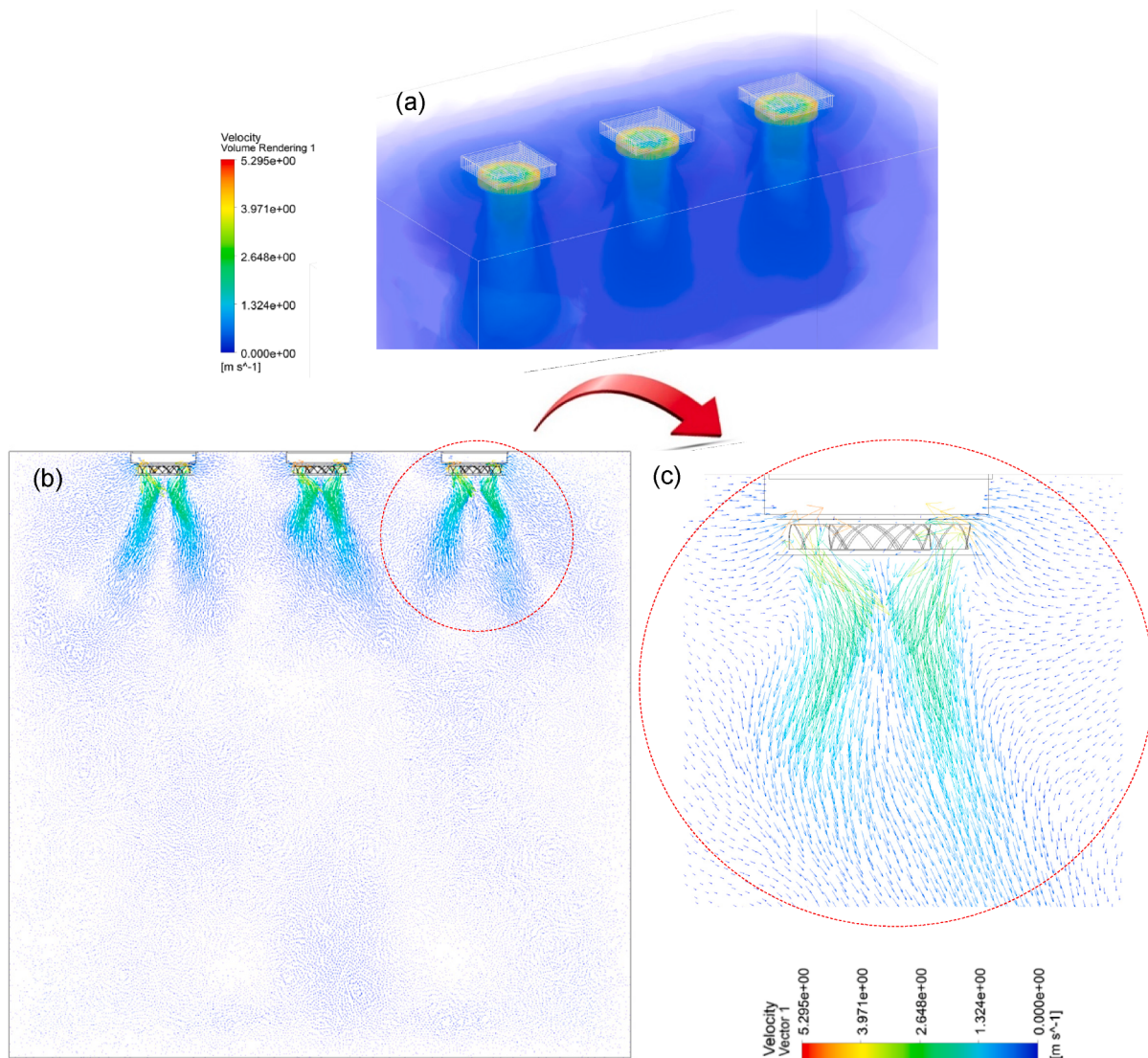


Fig. 11. (a) Velocity volume rendering results, (b) velocity vectors inside the cooling chamber and (c) velocity vectors around internal fans.

$V_{\text{air}} = 30 \text{ m/s}$), no significant effect was noted.

In Fig. 5, COP values, which is a measure of cooling performance, are presented for an analysis time of 1500 s. Here (a), (b) and (c) represent 4.5, 3.0 and 1.5 mm base thicknesses results, respectively. In these figures, the effects of external fan speeds of $V_{\text{air}} = 7.5, 15, 20$ and 30 m/s have been analyzed. Since the refrigerators operate in time dependent condition, COP value decreases depending on time and approaches zero in all obtained results. Considering achieved results in Fig. 5, the effect of external fan speeds on the COP value is quite strong at the beginning, but it weakens over time. The maximum COP value was obtained as 0.015 around the 50th second for 1.5 mm thickness and $V_{\text{air}} = 30 \text{ m/s}$ external fan speed.

In Fig. 6, the total cooling load is given for 4.5 mm heat exchanger base thickness. Here, the positive effect of air velocity on external exchanger is clearly seen. In this figure, the total Q_c value within the 1500 s analysis period, increased by 65% by increasing the external fan speed from $V_{\text{air}} = 7.5 \text{ m/s}$ to $V_{\text{air}} = 30 \text{ m/s}$.

Thermal imager results

Temperature contours were obtained in the laboratory conditions by a thermal camera during the test to determine the temperature distribution inside the cooling chamber and to evaluate the operation of the Peltiers, internal and external heat exchangers. Thermal camera image

of the experiment performed at the lowest external air velocity is illustrated in Fig. 7. And also the temperature variations on the specified lines P1 and P2 are presented in this figure. It can be seen that the warmest area is the external heat exchanger and its surroundings. The temperature gradient on the surface of external heat exchanger depends on the airflow from left to right.

Inhomogeneous temperature distribution inside the cooling chamber is due to the different performance of Peltier modules. The Peltier close to the air inlet in the external section works more effectively, due to the fact that the air on the external exchanger performs a more effective heat transfer. It can be concluded that, the temperature distribution on external exchanger has a notable influence on the Peltiers performance inside.

In Figure 8, thermal camera images are presented for different external fan speeds. As seen here, the heat exchanger surface temperature decreases strongly with the increase of the external fan speed. This situation (increasing fan speed) causes the Peltiers to work more efficiently, increasing the cooling rate. Due to the fact that the air flow blown by the external fan is from left to right, the temperature of the inlet region of the heat exchanger was lower as observed in the images.

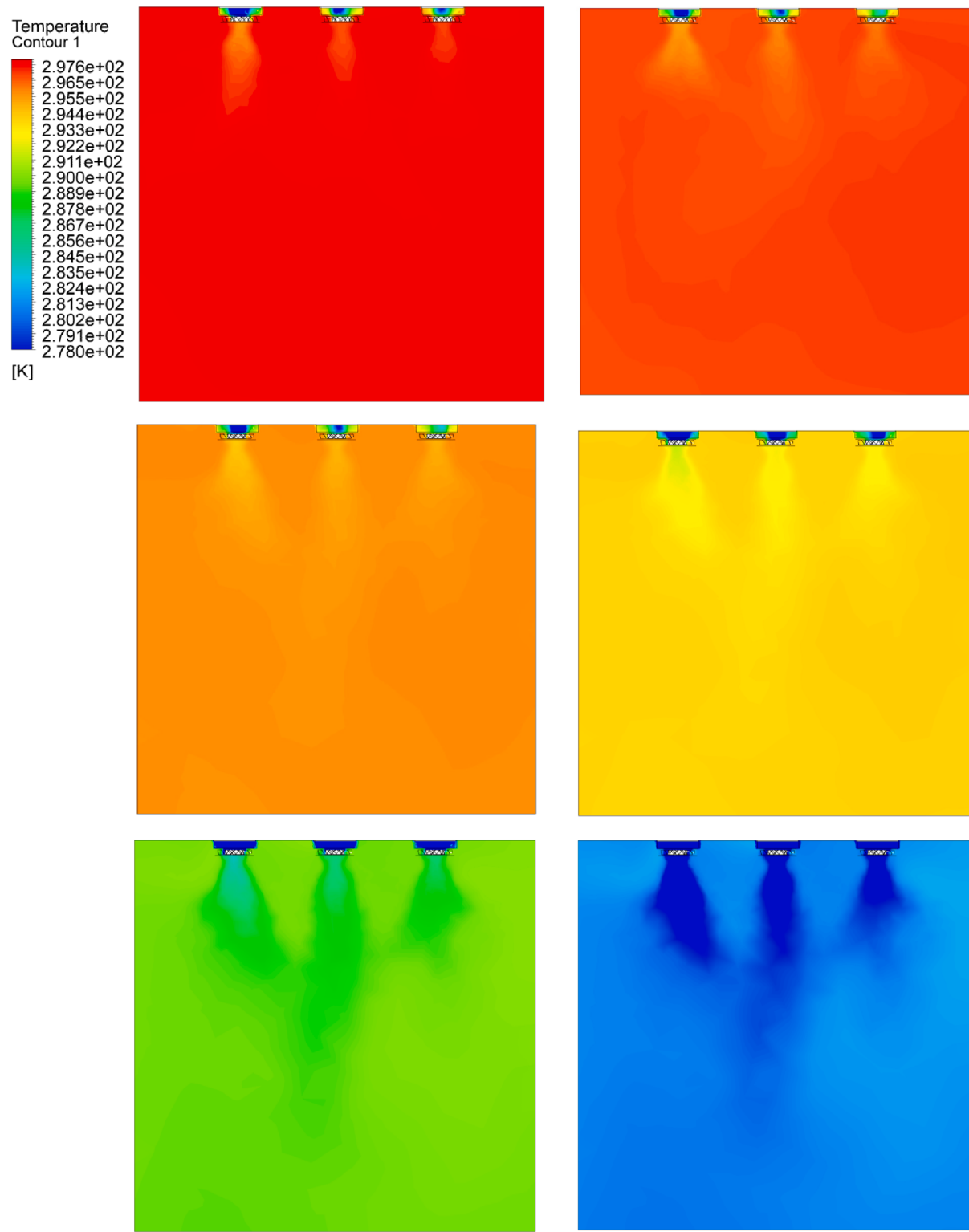


Fig. 12. Cooling trend during time inside the cooling chamber in 250 s intervals.

Numerical results

In this section, CFD results are presented in the form of contours for both cooling chamber and external heat exchanger. In Figure 9, temperature contours of the external fan and ambient air are given at 4 different air velocities. While the temperature gradients on the heat exchanger are larger at the lowest air speed, these gradients decrease as the air speed increases and the heat exchanger shows a more uniform

temperature distribution. As expected, the temperature of the entire domain (solid heat exchanger and ambient air) approaches the air inlet temperature with the increase in air velocity. These numerical results largely overlap with the thermal camera images given in Figure 8.

Additionally, in Fig. 10, temperature and velocity contours are also presented for the top view of the heat exchanger at the lowest air velocity $V_{\text{air}} = 7.5 \text{ m/s}$. In velocity contour it can be seen that velocity value around the exchanger is at highest levels and the vortex at the end

Table 2

COP results of refrigerators presented in literature.

Reference	Refrigerator type	Refrigerator capacity (cm)	Power supply	Application field	COP
Jugsujinda et al. (2011) [30]	Thermoelectric refrigerator	25 × 25 × 35	20–40 W	Prototype refrigerator	0.65
Abdul-Wahab et al. (2009) [6]	Thermoelectric refrigerator	23 × 18 × 32	9.5 W	Portable domestic refrigerator	0.16
Mirmanto et al. (2019) [31]	Thermoelectric refrigerator	215 × 175 × 130	38.08 W	Prototype refrigerator	0–0.025
Mirmanto et al. (2018) [32]	Thermoelectric refrigerator	285 × 245 × 200	1.04–38.76 W	Prototype cooler box	0–0.02
Caglar (2018) [33]	Thermoelectric refrigerator	60 × 40 × 27	Electrical energy	Prototype refrigerator	0.011–0.351
Martinez et al. [34]	Thermoelectric refrigerator	0.062 m ³	Electrical energy	Prototype refrigerator	0.09–0.33
Abderezzak et al. (2021) [35]	Thermoelectric refrigerator	30 × 30 × 24	–	Prototype refrigerator	0.2
Present Study	Thermoelectric refrigerator	0.022506 m ³	90 W	Prototype refrigerator	0–0.015

of heat exchanger is formed where the velocity value becomes smaller. The passage of air with a low velocity between the fins can be observed. This low velocity is due to friction with the fin walls. Passing through the fins, the air temperature at the end of the heat exchanger has increased significantly as shown in temperature contour. Thus, outlet temperature shows a further increase because of efficient heat transfer. Considering the temperature distribution on the aluminum exchanger, it can be stated that the areas close to the fan are cooled and have a lower temperature, but the end parts away from the fan are warmer and have the highest temperature.

With the aim of analyzing flow structure inside cooling chamber three-dimensional velocity volume rendering results around internal fans are given in Fig. 11(a). Heat dissipation and heat transfer by fans and forced heat transfer are very carefully considered in this present study. This subject is important in increasing the efficiency of the heat exchanger and the whole refrigerator system. For this reason, velocity vectors are provided inside the refrigerator, which can be seen in Fig. 11 (b). On the other hand, by enlarging the domain around the fan, the air circulation can be seen more clearly Fig. 11(c).

In Fig. 12, the temperature distributions of the cooling chamber are given in 6 stages (every 250 s). When the figure is examined in detail, it is seen that the Peltier in the inlet section of the external air, works more effectively in the first stages. The reason for this is that the temperature in the entrance area of the exchanger at the top is lower. However, in the following stages, it seems that the efficiency of the Peltiers converged due to the decrease in temperature of the cooling chamber and mixing effects and vortices inside the chamber.

In this section a literature review has been performed and it was found that COP value of refrigerators are notably low and it was seen that the ranges of the COP value of the whole system under different operating conditions are close to the similar studies in the literature. Table 2 summarizes presented articles in the literature to have a comparison with this present study.

Conclusion

In this work, a numerical and experimental study was carried out on multiple air-to-air Peltier cooling systems. An optimization treatment has been made on the subject that has been little studied in the literature and previous studies. This subject is the external heat exchanger base thickness and the air velocity passing over it. The experiments were performed on the heat exchanger base thickness and the air velocity at the top of the cooling chamber, and the values were evaluated for optimization and it was revealed that, the base thickness has a notable effect on the cooling performance and the greater the thickness of heat exchanger base leads to reduced efficiency. Therefore, in the design of the heat exchanger this thickness should be as small as possible. Considering the temperature results, it was observed that, by reducing the thickness from 4.5 mm to 1.5 mm for the case of $V_{air} = 7.5$ m/s external fan speed, a 14% improvement in the temperature drop of the refrigerator occurred. However, as the air velocity increases, the effect

of the base thickness decreases. COP values were taken into account and low COP values of these systems were revealed. The highest COP was obtained as 0.015. It was shown that, in refrigerators, the COP value decreases over time during the cooling period and approaches zero, which means that these systems work in time-dependent conditions. In this study, CFD results were presented to evaluate important points about heat transfer and flow structure by analyzing the velocity and temperature distributions in the solution domains.

This model can be further used to enhance the performance of the system. As an important factor heat exchanger design can be improved and accordingly heat transfer rate and total performance of the system can be increased. Additionally, the dimension of heat exchanger, fins arrangement, geometry and distance can be investigated and optimized.

Declaration of Competing Interest

The authors declare that they have no known competing financial interests or personal relationships that could have appeared to influence the work reported in this paper.

Acknowledgements

This project was supported by Research Project Foundation of the Erzurum Technical University (BAP Project No. 2020/10). The authors of this research gratefully acknowledge the support of this study.

References

- [1] Khanlari, A., Sözen, A., Sahin, B., Di Nicola, G., Afshari, F. Experimental investigation on using building shower drain water as a heat source for heat pump systems. *Energy Sour, Part A: Recov Util Environ Effects* 2020; 1–13.
- [2] Tan FL, Fok SC. Methodology on sizing and selecting thermoelectric cooler from different TEC manufacturers in cooling system design. *Energy Convers Manage* 2008;49(6):1715–23.
- [3] Drebushchak VA. The Peltier effect. *J Therm Anal Calorim* 2008;91(1):311–5.
- [4] Liu D, Zhao FY, Yang HX, Tang GF. Thermoelectric mini cooler coupled with micro thermosiphon for CPU cooling system. *Energy* 2015;83:29–36.
- [5] Zhou Y, Yu J. Design optimization of thermoelectric cooling systems for applications in electronic devices. *Int J Refrig* 2012;35(4):1139–44.
- [6] Abdul-Wahab SA, Elkamel A, Al-Damkhia AM, Al-Habsi IA, Al-Rubaiey HS, Al-Battashi AK, et al. Design and experimental investigation of portable solar thermoelectric refrigerator. *Renewable Energy* 2009;34(1):30–4.
- [7] Afshari F. Experimental and numerical investigation on thermoelectric coolers for comparing air-to-water to air-to-air refrigerators. *J Therm Anal Calorim* 2021;144(3):855–68.
- [8] Afshari F. Experimental study for comparing heating and cooling performance of thermoelectric Peltier. *Politeknik Dergisi* 2020;23(3):889–94.
- [9] Chen M, Lund H, Rosendahl LA, Condra TJ. Energy efficiency analysis and impact evaluation of the application of thermoelectric power cycle to today's CHP systems. *Appl Energy* 2010;87(4):1231–8.
- [10] Dai YJ, Wang RZ, Ni L. Experimental investigation on a thermoelectric refrigerator driven by solar cells. *Renewable Energy* 2003;28(6):949–59.
- [11] Gong T, Wu Y, Gao L, Zhang L, Li J, Ming T. Thermo-mechanical analysis on a compact thermoelectric cooler. *Energy* 2019;172:1211–24.
- [12] Tian X-X, Asaad S, Moria H, Kaood A, Pourhedyat S, Jermitsiparsert K. Proposing tube-bundle arrangement of tubular thermoelectric module as a novel air cooler. *Energy* 2020;208:118428.
- [13] Ali SA, Mazumder S. Computational study of transverse Peltier coolers for low temperature applications. *Int J Heat Mass Transf* 2013;62:373–81.

- [14] Martín-Gómez C, Zuazua-Ros A, Del Valle de Lersundi K, Sánchez Saiz-Ezquerro B, Ibáñez-Puy M. Integration development of a Ventilated Active Thermolectric Envelope (VATE): constructive optimization and thermal performance. *Energy Build* 2021;231:110593.
- [15] Liu Z, Zhang L, Gong G, Li H, Tang G. Review of solar thermoelectric cooling technologies for use in zero energy buildings. *Energy Build* 2015;102:207–16.
- [16] Manikandan S, Selvam C, Praful PPS, Lambari R, Kaushik SC, Zhao D, et al. A novel technique to enhance thermal performance of a thermoelectric cooler using phase-change materials. *J Therm Anal Calorim* 2020;140(3):1003–14.
- [17] Ismaila KG, Sahin AZ, Yilbas BS. Exergo-economic optimization of concentrated solar photovoltaic and thermoelectric hybrid generator. *J Therm Anal Calorim* 2021;1–18.
- [18] Liu H, Zhao X, Li G, Ma X. Investigation of a novel separately-configured micro-thermoelectric cooler to enabling extend application scope. *Appl Energy* 2022;306:117941.
- [19] Zhou Y, Yan Z, Dai Q, Yu Y. Experimental and numerical evaluation of a two-stage indirect/thermoelectric assisted direct evaporative cooling system. *Energy Convers Manage* 2021;248:114780.
- [20] Fang Z, Xie Y, Xu Y, Wu H, Zhang H, Han L. Performance investigation of a loop heat pipe integrated with thermoelectric cooler under acceleration field. *Int J Heat Mass Transf* 2021;178:121476.
- [21] Wang J, Wang J-b, Long Z-y, Zhu T, Li Z-S, Jiang Z-C, et al. Design and application of a cooling device based on peltier effect coupled with electrohydrodynamics. *Int J Therm Sci* 2021;162:106761.
- [22] Tuncer AD, Sözen A, Khanlari A, Amini A, Şirin C. Thermal performance analysis of a quadruple-pass solar air collector assisted pilot-scale greenhouse dryer. *Sol Energy* 2020;203:304–16.
- [23] Tuncer AD, Sözen A, Khanlari A, Gürbüz EY, Variyenli Hı. Upgrading the performance of a new shell and helically coiled heat exchanger by using longitudinal fins. *Appl Therm Eng* 2021;191:116876.
- [24] Çiftçi E, Khanlari A, Sözen A, Aytaç İ, Tuncer AD. Energy and exergy analysis of a photovoltaic thermal (PVT) system used in solar dryer: a numerical and experimental investigation. *Renewable Energy* 2021;180:410–23.
- [25] Gürbüz EY, Sözen A, Variyenli Hı, Khanlari A, Tuncer AD. A comparative study on utilizing hybrid-type nanofluid in plate heat exchangers with different number of plates. *J Braz Soc Mech Sci Eng* 2020;42(10):1–13.
- [26] Gelis K, Akyurek EF. Factorial design for convective heat transfer enhancement of hybrid nanofluids based on al 2 o 3-tio 2 in a double pipe mini heat exchanger. *Heat Transfer Res* 2021;52(15):41–62.
- [27] Yakut K, Sahin B, Celik C, Alemdaroglu N, Kurnuc A. Effects of tapes with double-sided delta-winglets on heat and vortex characteristics. *Appl Energy* 2005;80(1):77–95.
- [28] Pan L, Wang H, Chen Q, Chen C. Theoretical and experimental study on several refrigerants of moderately high temperature heat pump. *Appl Therm Eng* 2011;31(11–12):1886–93.
- [29] Sözen A, Gürü M, Khanlari A, Çiftçi E. Experimental and numerical study on enhancement of heat transfer characteristics of a heat pipe utilizing aqueous clinoptilolite nanofluid. *Appl Therm Eng* 2019;160:114001.
- [30] Jugusjinda S, Vora-ud A, Seetawan T. Analyzing of thermoelectric refrigerator performance. *Procedia Engineering*.
- [31] Mirmanto M, Syahru S, Wirdan Y. Experimental performances of a thermoelectric cooler box with thermoelectric position variations. *Eng Sci Technol*.
- [32] Mirmanto M, Sayoga I M A, Sutanto R, Alit I B, Nurchayati N, Mulyantao A. Experimental cooler box performance using two different heat removal units: a heat sink fin-fan, and a double fan heat pipe. *Front Heat Mass Transfer*.
- [33] Caglar A. Optimization of operational conditions for a thermoelectric refrigerator and its performance analysis at optimum conditions. *Int J Refrig*.
- [34] Martinez A, Astrain D, Rodriguez A, Aranguren P. Advanced computational model for Peltier effect based refrigerators. *Appl Therm Eng*.
- [35] Abderezzak B, Deepaul RK, Busawon K, Chabane D. Experimental characterization of a novel configuration of thermoelectric refrigerator with integrated finned heat pipes. *Int J Refrig* 2021;131:157–67.